



# Crater formation by ion bombardment as a function of incident angle

E.M. Bringa<sup>a,\*</sup>, E. Hall<sup>b</sup>, R.E. Johnson<sup>a</sup>, R.M. Papaléo<sup>c</sup>

<sup>a</sup> *Engineering Physics and Astronomy Department, University of Virginia, Charlottesville, VA 22903, USA*

<sup>b</sup> *The Research Computing Support Group, ITC, University of Virginia, Charlottesville, VA 22903, USA*

<sup>c</sup> *Faculdade de Física, Universidade Católica do Rio Grande do Sul, CP 1429, Porto Alegre, RS, Brazil*

---

## Abstract

Ion bombardment of surfaces at an angle with respect to the surface normal produces surface modification with more varied and rich features than normal incidence bombardment. This allows more possibilities for nanopatterning and surface processing. Megaelectronvolt ion bombardment of insulators can create a track of electronic excitations which can decay non-radiatively and couple to the lattice, leading to sputtering and crater creation. Using molecular dynamics simulations we present a systematic study of the craters produced by a cylindrical track of excitations with its axis at several angles with respect to the surface normal (in the range  $\Theta = 0\text{--}80^\circ$ ). We also use different energy densities inside the track, from  $0.5nU$  to  $12.5nU$ , where  $n$  is the density of the material and  $U$  its binding energy. Crater length is found to vary as  $\cos^{-1}\Theta$ . © 2002 Elsevier Science B.V. All rights reserved.

*PACS:* 79.20.A; 81.65.C; 34.50.Fa; 79.20.R

*Keywords:* Cratering; Angular dependence; Sputtering; Tracks; Molecular dynamics

---

## 1. Introduction

Cratering is a ubiquitous process occurring in nature and used in technology. In astronomical scenarios [1] crater radii vary from  $\mu\text{m}$  size for micrometeoroid impact up to thousands of kilometers for asteroid impact. Macroscopic projectile impact is used regularly to test materials strength, creating craters of the order of centimeters [2]. Small cluster impacts can create crater sizes from nanometers up to micrometers. Such processes

have been studied both experimentally [3,4] and extensively by simulations [5–8]. Crater formation by an individual fast ion impact has been seen experimentally in metals [9] and insulators [10], and has been reported in simulations of ion bombardment of metals [11,12], semiconductors [13] and insulators [14]. Most simulations deal with the energy deposition regime where nuclear energy loss dominates and they consider normal incidence or small angle incidence. There are a few recent experiments for oblique incidence onto solids composed of polymers [10] and biomolecules [15]. These were bombarded by fast heavy ions in the electronic energy loss regime, where the crater length was found to increase rapidly with increasing energy density.

---

\* Corresponding author. Tel.: +1-925-423-5724; fax: +1-925-423-7040.

E-mail address: [ebringa@llnl.gov](mailto:ebringa@llnl.gov) (E.M. Bringa).

In this paper molecular dynamics (MD) simulations are used to study the surface morphology produced by the energy deposited by fast ions incident at several angles with respect to the surface normal, and for several initial excitation densities. Since crater formation is used for nanopatterning [16], for determining surface properties [17] and for estimating sputtering yields [10,15], we use MD simulations to extract scaling laws for crater formation. Earlier we compared cratering in Lennard-Jones (L-J) solids to that observed experimentally in a polymer [18] for a fix angle of incidence. We showed that the scaling relationships are very similar in these materials suggesting that scaling laws which apply over a broad range of material properties can be found from simple interatomic potentials. Here the structure of craters formed from a track of energy deposited by a heavy ion is shown as a function of the incident angle and the results are compared to thermal spike model predictions [19].

## 2. Molecular dynamics simulation

Following the passage of a fast heavy ion a cylindrically energized region is produced in a solid, which we refer to as a track of excitations. A L-J crystalline solid is simulated with particles interacting through the potential [20]  $V(r) = 4\epsilon \left[ (\sigma/r)^6 - (\sigma/r)^{12} \right]$  with a cut-off radius  $r_{\text{cut}} = 2.5\sigma$  to describe an fcc atomic solid. Although this is an oversimplified model of a real solid, this two parameter potential has the advantage that the equations of motion, and, hence, all results, including the crater dimensions, scale with  $\epsilon$  and  $\sigma$ . In addition, certain weakly bound solids, such as the low-temperature, condensed-gas solids, can be reasonably approximated as L-J solids, with parameters  $\epsilon$  and  $\sigma$  taken to reproduce the material properties. All L-J samples have a cohesive energy  $U \approx 8\epsilon$ . The interlayer distance for (001) layers is  $d \approx 0.78\sigma$  and the bulk modulus is  $B = 75\epsilon/\sigma^3$ . More details on the MD simulation can be found elsewhere [20–22]. As in our earlier papers, the scaling with  $\epsilon$  and  $\sigma$  is replaced by scaling using  $U$  and the number density  $n$ . For the fast processes which determine sputtering and cratering we

showed that the scaling was roughly preserved when a more complex potential was used [23]. The melting temperature  $T_m$  of L-J solids at normal pressure is  $k_B T_m \approx 0.1U$ . At solid densities  $k_B T_m \approx 0.3U$ . For a number of condensed gas solids  $U \sim 0.1$  eV and  $\sigma \sim 3.5$  Å [23]. For fcc metals,  $U$  is of the order of few electronvolts and  $\sigma$  about 2 Å [24].

The stopping power, i.e. the energy deposited per unit depth into the solid  $dE/dx$ , and the track radius,  $r_{\text{cyl}}$ , are typically used to describe the energy density in the ion track. Since only a fraction of the experimental  $dE/dx$  goes into excitation of the particles in the track, in the following we use the symbol  $(dE/dx)_{\text{eff}}$  to represent the amount of energy deposition contributing to track formation, cratering and sputtering. To mimic the non-radiative energy release at the ion track in the MD simulations all  $N_{\text{exc}}$  particles within a cylinder of radius  $r_{\text{cyl}}$  are given an energy  $E_{\text{exc}}$  with their velocities in random directions. Therefore,  $(dE/dx)_{\text{eff}}$  is  $N_{\text{exc}}E_{\text{exc}}/d$ . As we have shown earlier this energized ‘track’ can be representative of either knock-on or electronic sputtering of a solid. A track radius can be estimated from the Bohr adiabatic radius in the electronic regime or from the cascade size in the nuclear regime, though this has been questioned recently [25,26]. At normal incidence the sputtering yield depends roughly linearly on the track radius. In this paper all simulations were run for an initial track radius  $r_{\text{cyl}} = 2\sigma$ , which implies  $N_{\text{exc}} \approx 10/\cos\theta$ . The incident angle,  $\theta$ , is measured in degrees with respect to the surface normal. The size of the simulated sample was varied depending on the size of  $E_{\text{exc}}$  such that the results did not depend on the boundary conditions used, and the total simulation time was also varied to be able to ‘detect’ all ejected particles. Most quantities presented are averages of results from a number of simulations (4–30) in which the directions of the energized atoms were randomly varied. We studied the yield from a [001] surface. The small focused collision component of the ejecta, discussed earlier [27], will differ for different crystallographic surfaces. However, earlier we showed that the total sputtering yields from other crystallographic orientations have the same dependence on  $(dE/dx)_{\text{eff}}$  [21]. Therefore, we presume the cratering is not very sensitive to the crystal orientation. The energized

tracks were directed along the  $\langle 100 \rangle$  direction in the  $xy$  plane. Some simulations were run rotating the beam so it would not be directed along any low index crystallographic direction. Crater size was not affected significantly within the standard error.

The mass of the simulated particles,  $M$ , only changes the time scale, which is given in units of  $t_0 = \sigma\sqrt{M/\epsilon}$ . Simulations were run during  $\sim 15$ –

$75t_0$ , well after all the sputtering ended to account for possible late relaxation. We double the simulation times in several cases and found no difference in the crater structure. The temperature of the target at the end of the simulation was well below the melting temperature. Relaxation over much longer times (hundreds or thousands of  $t_0$ ) could occur but this is beyond the abilities of MD sim-

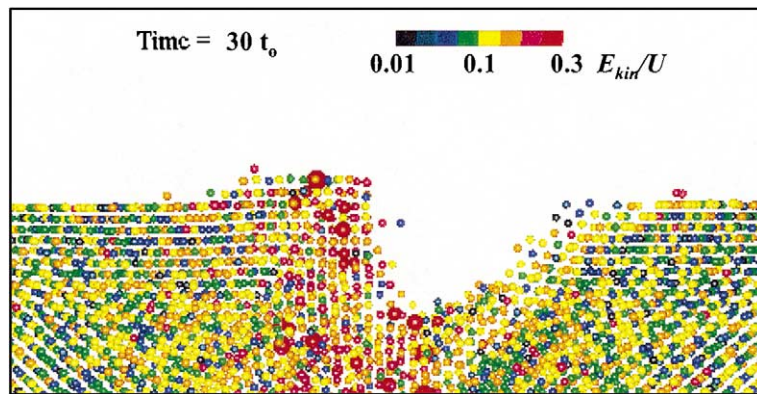


Fig. 1. Snapshot showing a side view of a central slice from the MD simulation.  $\Theta = 60$  and  $E_{exc} = 12.5U$ . Notice the crater rim above the original surface. Logarithmic color scale indicates kinetic energy. The size of the atoms also increases logarithmically with their kinetic energy to help the visualization of ‘hot’ atoms.

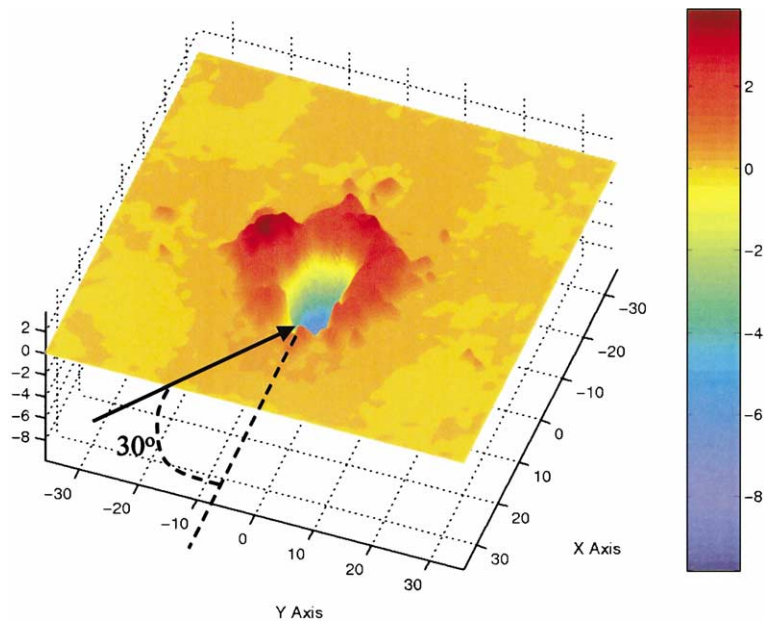


Fig. 2. Perspective view of a crater shown in Fig. 1, indicating the incident ion as an arrow. Color scale indicates height. Notice the crater rim in red above the original surface.

ulations, although it could occur in an experimental setting.

### 3. Cratering

Fig. 1 shows a central slice of the MD simulation for  $\Theta = 60$  and  $E_{\text{exc}} = 12.5U$ ,  $30t_0$  after bombardment [28]. Note that the crater is not well approximated by a half ellipsoid, since its depth profile is slanted towards the ion incident direction. Therefore, estimates of crater volume must be made carefully. Although a few individual atoms are still ‘hot’, we find that the crater walls are below the melting temperature and, therefore, are not likely to relax substantially, as was verified by running this simulation until  $60t_0$  after excitation. The topography of the bombarded surfaces was obtained from the MD configuration  $xyz$  snapshots using a Matlab [29] routine which one of us (E. Hall) developed. The details of the routine, where to download and how to use it, will be discussed in an upcoming paper [30]. Fig. 2 shows a perspective view of the crater in Fig. 1 obtained using this routine.

The area of the crater is roughly circular at normal incidence and  $E_{\text{exc}} \gg U$ . As the angle is increased the area becomes roughly elliptical, with the major axis of the ellipse along the direction of incidence of the ion. This major axis is used to define the crater length in the discussion below. The length of the crater as a function of the incident angle is shown in Fig. 3 for several excitation energies. It can be seen that the data closely follow a  $\cos^{-1} \Theta$  at each excitation energy. This is the same region of energy density in which we earlier showed that the size of the ejecta (sputtering) yield depends nearly linearly on energy density and also varies as  $\cos^{-1} \Theta$ . We normalized the crater length to the length at  $\Theta = 0$  for each set of data corresponding to a given  $E_{\text{exc}}$  and then fit the data for  $E_{\text{exc}} > U$  with the function  $\cos^x \Theta$ . The best fit is given by  $x = -0.99 \pm 0.02$ . The results for runs with  $E_{\text{exc}} = U$  were excluded because no crater is formed until  $\Theta = 75$ . These simulations are at the boundary between the linear regime for sputtering, mentioned above, and the threshold regime where the yield steeply decays with decreasing energy

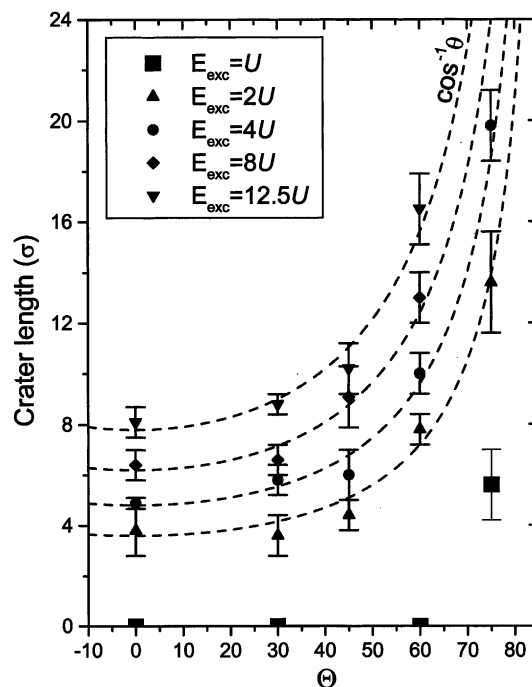


Fig. 3. Crater length as a function of  $\Theta$  for different excitation energies. Dashed lines are of the form  $C \cos^{-1} \Theta$  with  $C$  a constant.

density [23]. The  $\cos^{-1} \Theta$  dependence found here agrees with the prediction of a simple thermal spike model for cratering by a heated cylindrical track [19]. The agreement may be coincidental, since the MD results for the sputtering yield at an angle does not follow thermal spike model predictions [22].

### 4. Discussion and summary

We carried out a series of MD simulations to study crater formation due to the high energy density deposited in a cylindrical ‘track’. Such an energized track might be formed by a penetrating fast ion that deposits its energy in electronic excitations, which is of interest here, or deposits its energy by momentum transfer producing recoil atoms. That is, the craters described are not impact craters like the lunar craters [1] formed by the direct transfer of projectile momentum to the lunar surface, rather they are the craters formed in

response to the rapid energy deposition in the track of an energetic ion which produces an outward and radial pressure pulse. The study here covers different angles of incidence, from normal incidence to  $80^\circ$  respect to the surface normal, and also spans different excitation energies,  $E_{\text{exc}}$ , inside the ion track, from below the binding energy to more than 10 times the binding energy.

The crater structure remains stable in this L-J material over the longest simulation time tested ( $\sim 75t_0$ ), which is much larger than the crater formation time ( $\sim 20t_0$ ). This is the case because of the rapid cooling of the track by the melting and pressure pulse processes described in earlier papers [21,31]. No crater is formed at energies per L-J particle below the binding energy  $U$ . When  $E_{\text{exc}} = U$  no crater is formed except at the largest incident angle studied here. Above this energy, the crater length has a  $\cos^{-1} \theta$  dependence with the incident angle for a fix excitation energy. This is in agreement with predictions of a thermal spike model [19]. However, such models have no direct way of determining the structure of craters with rims. In addition, previous studies of the sputtering yield at an angle [22] and some preliminary results on crater width and volume do not follow the predictions of this model. A paper is in preparation comparing the sputtering yields and crater volumes.

## Acknowledgements

This work was supported by the National Science Foundation Astronomy and Chemistry Divisions.

## References

- [1] D. Gault et al., *J. Geophys. Res.* 80 (1975) 2444.
- [2] S.A. Quinones, L.E. Murr, *Phys. Stat. Sol. (a)* 166 (1998) 763.
- [3] I. Yamada et al., *Mater. Sci. Engng. A* 253 (1998) 249.
- [4] H.H. Andersen et al., *Phys. Rev. Lett.* 80 (1998) 5433.
- [5] M. Ghaly, R.S. Averback, *Mater. Res. Soc. Symp. Proc.* 279 (1992) 17.
- [6] M. Moseler, J. Nordiek, H. Haberland, *Phys. Rev. B* 56 (1997) 15439.
- [7] R. Aderjan, H.M. Urbassek, *Nucl. Instr. and Meth. B* 163–164 (2000) 697.
- [8] Z. Insepov, R. Manory, J. Matsuo, I. Yamada, *Phys. Rev. B* 61 (2000) 8744.
- [9] R.C. Bircher, S.E. Donnelly, *Nucl. Instr. and Meth. B* 148 (1999) 194.
- [10] R.M. Papaléo et al., *Nucl. Instr. and Meth. B* 148 (1999) 126.
- [11] R.S. Averback et al., *Mater. Res. Soc. Symp. Proc.* 396 (1996) 3.
- [12] E.M. Bringa, K.H. Nordlund, J. Keinonen, *Phys. Rev. B* 64 (2001) 235426.
- [13] K. Kyuno et al., *Phys. Rev. Lett.* 83 (1999) 4788.
- [14] D. Fenyő, R.E. Johnson, *Phys. Rev. B* 46 (1992) 5090.
- [15] J. Eriksson et al., *Int. J. Mass Spectrom. Ion Processes* 175 (1998) 293.
- [16] A. Quist et al., *J. Colloid Interf. Sci.* 189 (1997) 184.
- [17] R.M. Papaléo et al., *Phys. Rev. B* 62 (2000) 11273.
- [18] E.M. Bringa, R.M. Papaléo, R.E. Johnson, *Phys. Rev. B* 65 (2002) 094113.
- [19] C.T. Reimann, *Nucl. Instr. and Meth. B* 95 (1994) 181.
- [20] E.M. Bringa, R. Johnson, *Nucl. Instr. and Meth. B* 143 (1998) 513.
- [21] E.M. Bringa, R. Johnson, L. Dutkiewicz, *Nucl. Instr. and Meth. B* 152 (1999) 267.
- [22] E.M. Bringa, R. Johnson, *Nucl. Instr. and Meth. B* 180 (2001) 99.
- [23] E.M. Bringa, R.E. Johnson, M. Jakas, *Phys. Rev. B* 60 (1999) 15107.
- [24] K. Barghorn, E.R. Hilf, *Nucl. Instr. and Meth. B* 88 (1994) 196.
- [25] E.M. Bringa, R.E. Johnson, *Surf. Sci.* 451 (2000) 108.
- [26] P. Sigmund, *Nucl. Instr. and Meth.* 164–165 (2000) 401.
- [27] E.M. Bringa, *Nucl. Instr. and Meth. B* 153 (1999) 64.
- [28] Figures of several craters, including 3D views, available from <http://dirac.ms.virginia.edu/~emb3t/craters/craters.html>.
- [29] Matlab's web site: <http://www.mathworks.com/products/matlab/>.
- [30] E. Hall, E.M. Bringa, in preparation.
- [31] M.M. Jakas, E.M. Bringa, *Phys. Rev. B* 62 (2000) 824.